Dielectric Spectroscopy of Conductive Polyaniline Salt Films

MOON GYU HAN, SEUNG SOON IM

Department of Fiber and Polymer Engineering, Division of Chemical Engineering, Hanyang University, Seoul 133-791, South Korea

Received 2 January 2001; accepted 1 February 2001

ABSTRACT: Dielectric responses of polyaniline (PANI) salt films, made from two different methods, were compared to investigate the effect of a dopant and film-formation methods on the dielectric properties. One of the film-formation methods for emeraldine salt was the film-doping method, and the other, the solution-doping method. The conductivity relaxation and dielectric properties were measured by a microdielectrometer at 293 K in the frequency range of 1–100,000 Hz. Dielectric spectra were a function of the dopant in the case of the film-doping method, whereas it was a function of solvent–dopant combinations as well as the dopants in the solution-doping method. The dielectric responses of film-doped samples had similar patterns irrespective of the dopants, while those of solution-doped samples were varied, probably due to different conjugation conditions or/and the conduction mechanism. In the case of film-doped samples, dielectric loss and permittivity values were increased with decreasing dopant sizes. The dielectric relaxation times were also varied depending on the kind of dopants. The different solvent–dopant combinations led to variation of the dielectric responses in the solution-doped PANI due to an altered chain structure. © 2001 John Wiley & Sons, Inc. J Appl Polym Sci 82: 2760–2769, 2001

Key words: polyaniline; dielectric properties; electric modulus; conductivity relaxation

INTRODUCTION

Conducting polymers, which contain conjugated double bonds, have been intensively investigated due to their increasing applications.[1–4] For application of conducting polymers, knowing how the conducting material will affect the behavior in an electric field is a long-standing problem and of great importance. But little is known about the dielectric properties of conducting polymers associated with the conducting mechanism. The charge-transport mechanism of conducting polymers has been investigated in recent years using dielectric relaxation behavior and ac conductivity measurements, etc.[5–9] Dielectric spectroscopy has been found to be a valuable experimental tool for understanding the phenomenon of charge transport in conducting polymers.[10,11] Low-frequency conductivity and dielectric relaxation measurements especially have proven to be valuable in giving additional information on the conduction mechanism that dc conductivity measurement alone does not provide.

It is known that the dc electrical conduction of slightly doped and barely doped polyaniline

Correspondence to: S. S. Im (imss007@email.hanyang.ac.kr).

Contract grant sponsor: Center for Advanced Functional Polymers of the Engineering Research Center, Republic of South Korea.

Journal of Applied Polymer Science, Vol. 82, 2760–2769 (2001)

(PANI) is ensured by a mechanism of a variable-range hopping transport of carriers.[12,13] Polarons and bipolarons, made by proton doping in a specific configuration of a double bond between nitrogen and carbon atoms within a conjugation chain, have been suggested to be dominant charge carriers. In the case of highly doped PANI, it has been assumed that the growing dc conductivity is due to the appearance of a quasi-metallic zone, where the electrical charge is delocalized over the conjugated chains.[14,15] It has also been shown that the relaxation of an electric field in a charge-carrier system is attributable to the charge hopping of mobile carriers, which can lead to both short-range (or local) ac conductivity and long-range dc conductivity.

The conductivity relaxation in conjugated polymers, arising from carrier hopping (dc conductivity), can be inferred from complex dielectric permittivity as it takes into account conductivity and dielectric polarization. It depends on the frequency, as various mechanisms responsible for polarization exist in different ranges of frequencies. Hence, study of the frequency dependence for the dielectric behavior of materials will give information about the electrical properties of materials. Studies on the dielectric properties of PANI have been directed mainly to defining the conduction mechanism in the dedoped or slightly doped form as mentioned above. The dielectric behavior would also vary with the dopants, chain structure, and doping level, etc. It must also be greatly affected by the film-formation method and the selection of the dopant and solvent. Hence, here we report on observations of the dielectric properties of PANI salt films made by two different methods to define the role of the dopant and the chain structure on the dielectric properties. One method was doping PANI emeraldine base film in a 0.5*M* dopant solution and the other was preparing PANI-complex films from solvent using counterion-induced processability.[16,17]

EXPERIMENTAL

Chemicals

Aniline (from Aldrich Co.) was purified by distillation in a vacuum before use. Ammonium peroxydisulfate [$(NH_4)_2S_2O_8$], working as an oxidant, and NH_4OH, for the deprotonating agent, were used as received. Doping reagents such as HCl, camphorsulfonic acid (CSA), and dodecylbenzenesulfonic acid (DBSA, from Kando Chemical, Seoul, South Korea) were also used as received. *N*-Methyl-2-pyrrolidinone (NMP), xylene, and *m*-cresol used as solvents for the solution process were used as received.

Preparation of PANI Salt Films

PANI emeraldine base (EB) powder was chemically synthesized by the oxidative polymerization of aniline in a 1*M* aqueous HCl solution with $(NH_4)_2S_2O_8$ as the oxidant, as described in our previous works[16,17] and similar to the method used by MacDiarmid et al.[18] To obtain the base form, the powder was stirred for 12 h in a 0.1*M* aqueous solution of ammonium hydroxide, then washed with water several times, and finally dried under a vacuum by P_2O_5 in a desiccator. Then, about a 100-μm thickness of PANI–EB film was prepared by casting with the solvent (NMP) containing a 1 wt % PANI–EB solution onto a Petri dish. PANI–CSA, PANI–DBSA, and PANI–HCl films were prepared by immersing the PANI–EB film into 1*M* CSA, DBSA, and HCl aqueous solutions, respectively, for 8 h. This method will be designated as the film-doping method hereafter. The solution-doping method is as follows: CSA-doped PANI (PANI–CSA) and DBSA-doped PANI (PANI–DBSA) films from *N*-methyl-2-pyrrolidinone (NMP) were prepared as previously reported.[16,17] To compare the solvent effect, PANI–CSA and PANI–DBSA were dissolved in *m*-cresol and xylene, respectively. After these solutions with proper weight ratios were stirred for 24 h, they were poured into a Petri dish. Free-standing films were obtained by solvent casting the solution, then putting them in a vacuum-drying oven (50°C for NMP and 30°C for xylene) for over 1 day depending on the solvent. When the solvent was *m*-cresol, a PANI–CSA(*m*-cresol) solution was placed under hood for 1 day to obtain the film.

Measurements

The dielectric properties of samples were measured by a Eumetric System III microdielectrometer (1–10^5 Hz) to measure the dielectric constant and dielectric loss factor. A midconductivity interdigitated electrode sensor (IDEX) was used to collect dielectric responses of the samples. The sensor was made from a nickel-plated copper electrode to prevent electrode polarization from occurring readily. Rectangular samples over

0.325 in. in width and 1 in. in length were contacted onto the 1 × 0.325 × 0.006 in.-sized IDEX sensor surface. The experimental temperature was fixed at 293 K. The dielectric responses in the higher-frequency region were determined over a frequency range of 10 kHz to 10 MHz using an HP4274 LCR meter. For these measurements, thin gold layers were vacuum-evaporated on their surfaces as electrodes by a plasma-enhanced chemical vapor-deposition system. Wide-angle X-ray diffraction patterns were obtained by a Rigaku Model D/Max-2000. The scattering-angle ranges were 2°–40°. The X-ray source was 40 kV and 100 mA with Cukα radiation (λ = 1.54Å) generated from a rotating anode source, which was monochromatized by a crystal monochrometer.

RESULTS AND DISCUSSION

In Figure 1, the measured real part of complex permittivity ε' (relative permittivity or dielectric constant) and the imaginary part of complex permittivity ε'' (dielectric loss factor) of PANI films prepared by the film-doping method are plotted as a function of the frequency. A relatively high dielectric constant at low frequency and a fast decrease with the frequency are characteristics of a conducting polymer and consistent with other reports.[19,20] ε' exhibits a low-frequency plateau corresponding to the bulk static dielectric constant ε_0 and then decreases with increasing frequency, finally forming low-value plateau ε_∞ at the higher-frequency region. ε'' shows a loss peak characterized by a relaxation frequency for all samples. The peak maximum frequency f_{max} of PANI films seem to occur concomitantly with a sudden decreasing of ε' values which are not masked by dc conduction. After the loss factor reaches f_{max}, it decreases almost linearly in all samples and the position of f_{max} of ε'' is dopant-dependent. The increase in dopant sizes (from HCl through CSA to DBSA) results in subsequent displacement of the relaxation curve maximum toward lower frequencies (f_{max} = 200, 20, and 2 Hz, respectively), which means a corresponding increase of relaxation times. The relaxation times are $\tau = 1/(2\pi f_{max})$, 7.96 × 10^{-4}s, 7.96 × 10^{-3}s, and 7.96 × 10^{-2}s, respectively.

The difference in the dielectric relaxation times with the dopants may be due to the electric charges being displaced inside the polymer (stronger localization) and/or their lower concentration. Two possible causes can exist: The first is that the increase in the counteranion size led to an increasing interchain distance, which makes hopping between chains more difficult and, hence, resulting in a reduction of conductivity. Another possible assumption can be different doping levels depending on the dopants. Small molecules such as HCl would approach the quinoid imine nitrogen easier than would the other dopants and, hence, can lead to higher doping levels. Anyway, the dielectric relaxation time variation with the dopant may be in accord with the electrical conduction because, in theory, a relation exists between σ and $e_0\omega\varepsilon''$, where σ is the conductivity, $\omega = 2\pi f$ (f is the measuring frequency), and e_0 is the free-space permittivity (8.854 = 10^{-14} F/cm).

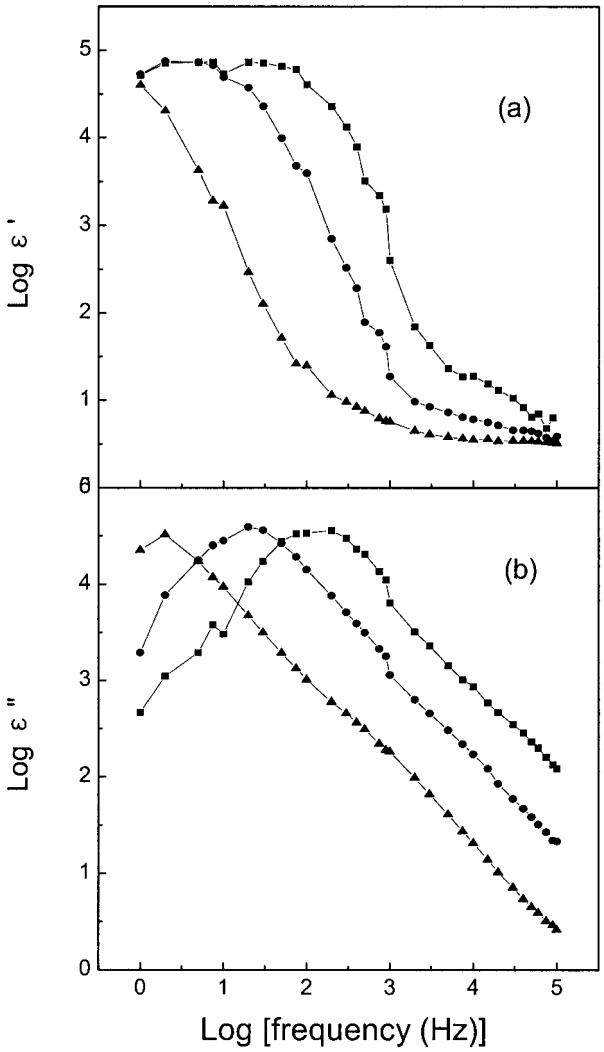

Figure 1 Frequency dependence of (a) dielectric constant (ε') and (b) dielectric loss factor (ε'') for film-doped PANI with (■) HCl, (●) CSA, and (▲) DBSA.

As ε' represents the capacitance nature and ε'' represents the conductive nature, the electrical behavior of the sample can be traced by elucidating the dielectrical behavior involving ε' and ε'' from the complex permittivity ε^*, which consists of ε' (real part) and ε'' (imaginary part) as

$$\varepsilon^*(\omega) = \varepsilon'(\omega) - i\varepsilon''(\omega) = \varepsilon'(\omega) - i[\sigma(\omega)/e_0\omega] \quad (1)$$

Hence, it can be deduced from this concept that the electrical conduction most readily occurs in HCl-doped PANI as analyzed from the ε'' data after reaching its maximum value in Figure 1(b). The need for careful observation of the electrical and dielectrical behavior made us use the dielectric relation formula modified from Hourquebie and Olemo[21]:

$$\varepsilon''_{f(\mathrm{Hz})} = \varepsilon''_{200\mathrm{Hz}} \times f^{-S} \quad (2)$$

Because all the experimental ε'' curves have linear relations in the range of 200–100,000 Hz, this formula is convenient for calculating the value of ε'' for this frequency range. Calculated s values of PANI–HCl, PANI–CSA, and PANI–DBSA by linear fit are 0.92, 0.94, and 0.87, respectively. As ε'' would be proportional to the conductivity of the materials, the relationship between σ and ε'' should exist theoretically. Thus, the conductivity σ would be nearly $\sigma \propto f^{-0.9}$ in all samples, that is, the conductivity should increase with a decreasing frequency, which indicates that the electron motion in PANI salt was performed by the way of jumping (carrier hopping).[22]

The hopping of charge carriers can make a great contribution to ε' and ε'', which are related both to dielectric characteristics such as a jumping dipole in its reciprocating motions and to conductive characteristics. The similar s values irrespective of dopants may be arise from similar chain structures because these films were made from the same PANI–EB film even though the chain structure might be slightly changed after protonation with different dopants because of different molecular sizes and protonation ability. The doping level does not seem to contribute to the variation of the dielectric responses because a change in the doping level should alter the s values.[21] Therefore, it is more persuasive that increasing the counteranion size increases the interchain distances of PANI. The capacitive couplings between chains are then lowered as observed by a weaker ε' value for PANI doped by a larger molecule. In a similar way, when the interchain distance increases, hops between chains become more difficult; then, the ε'' decreases, which is indicative of a conductivity decline.

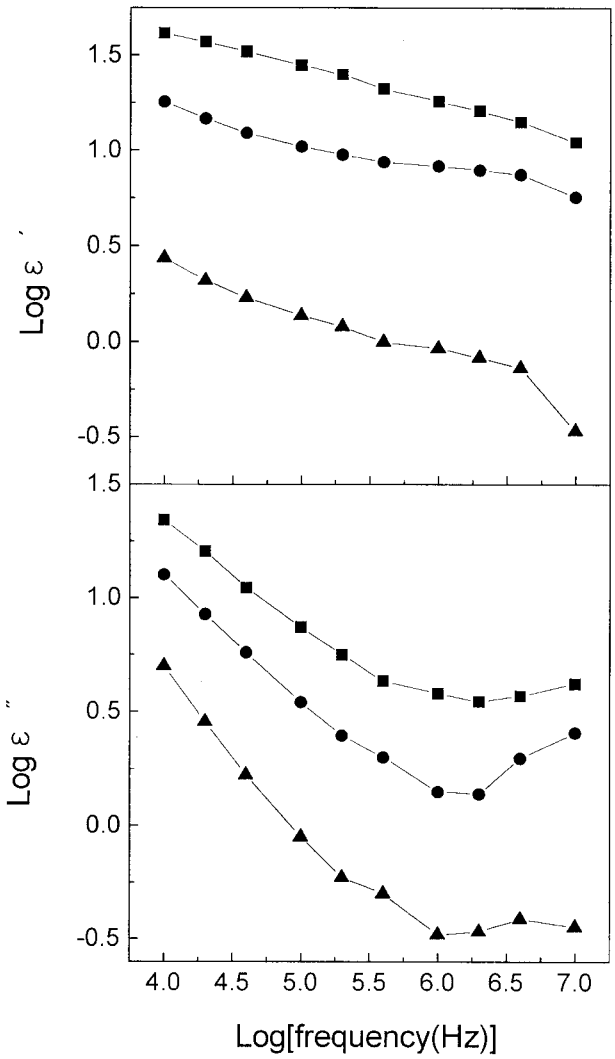

Figure 2 High-frequency spectra of (a) dielectric constant (ε') and (b) dielectric loss factor (ε'') for film-doped PANI with (■) HCl, (●) CSA, and (▲) DBSA.

In the higher-frequency measurements (10 kHz–10 MHz), although the measuring condition was different in that it measured the volume characteristics, on both sides of the PANI film from a surface measurement of low-frequency measurements, the measured s values are different from those calculated from Figure 2. The values are 0.38, 0.48, and 0.59, respectively, for HCl-, CSA-, and DBSA-doped film. This large difference in the s value, in comparison with the low-frequency measurement, may lie in the different

measuring methods (surface measurement for low-frequency data and bulk measurement for high-frequency data). The doping levels of the surface environment have similar values without regard to the dopant, while those of volume environments should be different because of different diffusivities of the dopant to the core of the film. This result indicates that the smaller dopant molecule diffuses more easily into the inside of the PANI film than does the larger dopant. On the surface, on the other hand, the dopant sizes have little influence on the doping level. This result supports the above-mentioned suggestion that the relaxation-time divergence should be dependent on the interchain distance on the surface.

To analyze the conductivity relaxation property in more depth, the complex permittivity (ε^*) is converted to the complex electric modulus $M^*(\omega)$, according to the relation mentioned by Macedo et al.[23] because ε^* is not completely suitable to describe the electrical properties of conjugated polymers. The real and imaginary parts M' and M'' of the electric modulus can be calculated from ε' and ε'' as follows[24]:

$$M' = \varepsilon'/(\varepsilon'^2 + \varepsilon''^2)$$

$$M'' = \varepsilon''/(\varepsilon'^2 + \varepsilon''^2) \quad (3)$$

The complex electric modulus $M^*(\omega)$ is also expressed by

$$M^*(\omega) = M'(\omega) + iM''(\omega) \quad (4)$$

$M^*(\omega)$ characterizes the dynamic aspects of the charge motion in conductors in terms of a relaxation in an electric field. Hence, this electric modulus description can explain the dispersion of ε^* with the frequency without any "molecular" polarizaion phenomena. From the M' and M'' of the PANI–dopants shown in Figure 3, the dispersions of M' and M'' indicate the presence of the relaxation-time distribution of conduction. M' in Figure 3(a) approaches zero at low frequencies, indicating that the electrode polarization gives a negligible low contribution to M' and can be ignored when the permittivity data are expressed in this form.[25] After keeping a low value, M' steeply increased after 50, 500, and 2000 Hz, respectively, for PANI–DBSA, PANI–CSA, and PANI–HCl. This is more evident in the inset of Figure 3(a) presented in a log scale. Figure 3(b) shows the frequency dependence of the imaginary part of

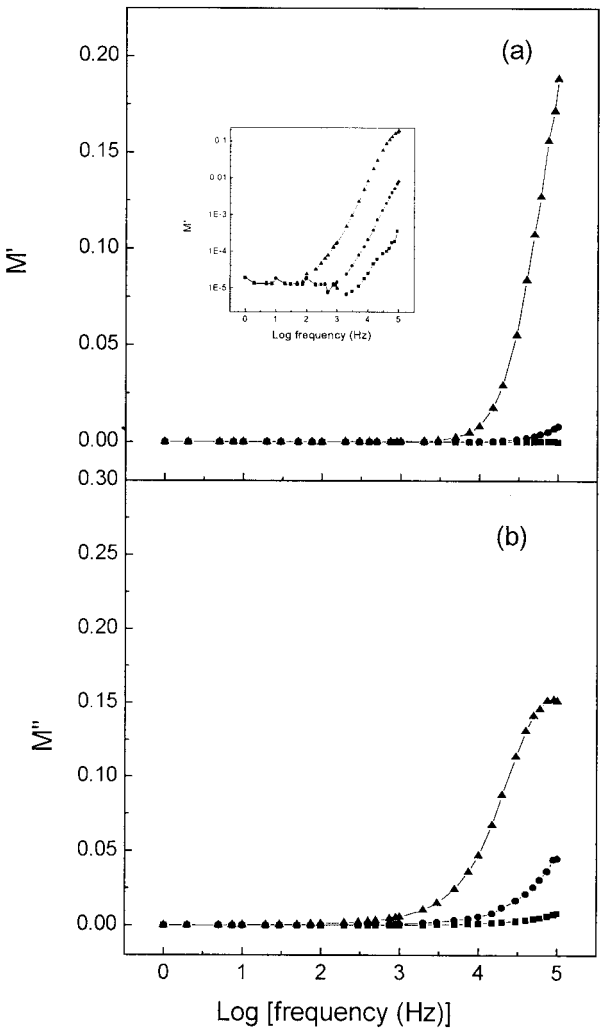

Figure 3 Electric modulus of (a) real part (M') and (b) imaginary part (M'') versus frequency for film-doped PANI with (■) HCl, (●) CSA, and (▲) DBSA.

the electric modulus doped with three different dopants. The peak maximum of the M'' curve seems to be located beyond the interval of frequencies used in these measurements. But, as expected, PANI doped by DBSA seems to have a maximum M'' in these frequency regions (about 100 kHz), while the M'' maximum of the HCl-doped PANI was located over 10 MHz by high-frequency measurements. Although the method is different and the resulting information would be different, it informs us that the increase in the dopant size leads to the appearance of M'' in the higher-frequency regions, which means enhanced dc conductivity, as predicted in theory that the maximum M'' is moving toward higher frequency according to the following expression:

$$\sigma_{dc} = e_0/(M_\infty\langle\tau\rangle) \quad (5)$$

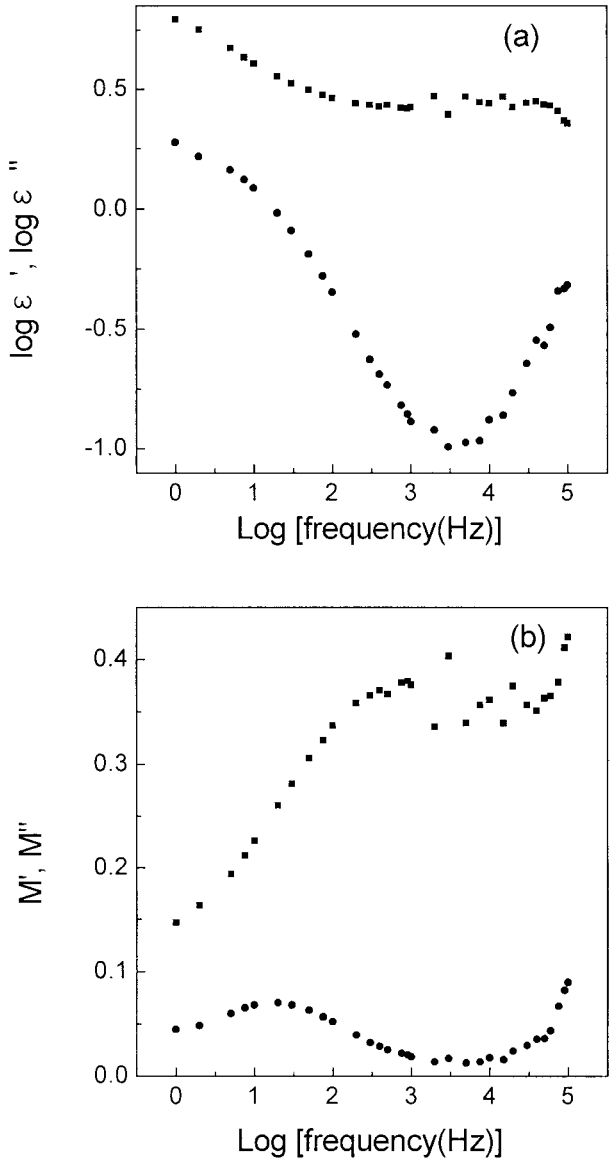

Figure 4 (a) Log frequency versus log ε' and log ε''. (b) Log frequency versus M' and M'' of PANI–EB.

where M_∞ is the high-frequency limit of the inverse ε' ,defined as $M_\infty = 1/\varepsilon_\infty$ and $\langle\tau\rangle$ is the relaxation time calculated from $\langle\tau\rangle = \frac{1}{2}\pi f_{max}$.

The intensity of the electric modulus seems to be inversely dependent on the dc conductivity. To support these results, the dielectric spectra and the electric modulus spectra of PANI–EB are shown in Figure 4. In the dedoped state, the observed ε' and ε'' values are relatively low and the M'' relaxation peak is seen in the measured frequency range (located at about 10 Hz), as shown in the electric modulus spectra in Figure 4(b). This coincides well with the results of Lee et al.[26]

As a result of doping, this peak shifts toward higher frequencies with increasing dc conductivity.

Figure 5 shows (a) tan δ curves and (b) the complex plane of M' and M''. The maximum of the tan δ curves shifts toward lower frequencies with increasing dopant size. The tan δ maximum is situated nearly at the f_{max}, which coincides with the subsequent increase in conductivity with decreasing dopant size. The complex plane diagrams for the electric moduli [Fig. 3(b)] are the

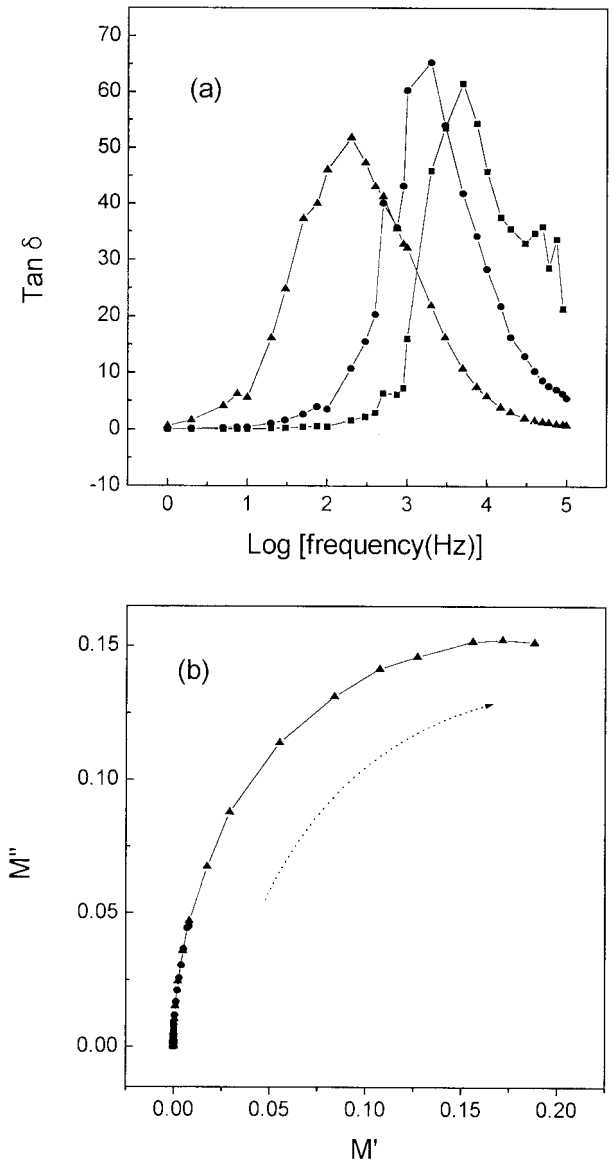

Figure 5 (a) Tan δ curve of film-doped sample: (■) HCl; (●) CSA; (▲) DBSA. (b) Complex plane for the electric modulus of film-doped sample: (■) HCl; (●) CSA; (▲) DBSA.

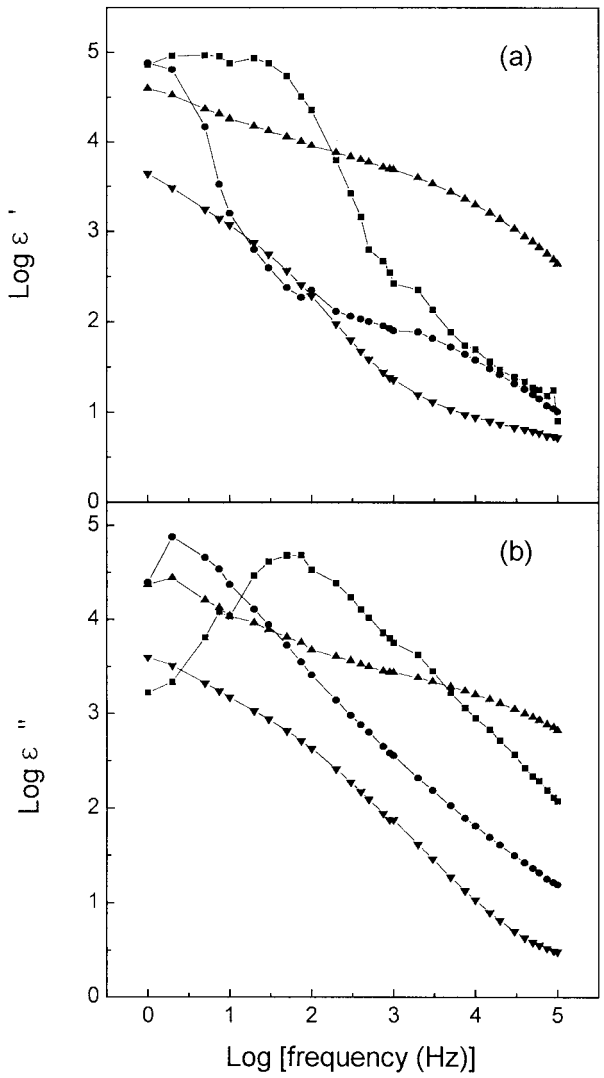

Figure 6 Frequency dependence of (a) dielectric constant (ε') and (b) dielectric loss factor (ε'') for solution-doped PANI with (■) CSA–*m*-cresol, (●) CSA–NMP, (▲) DBSA–xylene, and (▼) DBSA–NMP.

arcs with their centers and the radii of the arcs seem to be the same. Matveeva[19] reported that the radius of the arc of the complex plane diagram is dependent on the electrical conductivity of the samples, that is, the larger arc means lower electrical conductivity. In our case, although our samples have different conductivities, the complex diagrams have the same radius of the arc, showing only a difference in the length of the arc. This plot then allows the different curves to fit the same arc, which means a similar chain structure, irrespective of the kinds of dopants and the conduction that occurred.

Figure 6 shows log (ε') and log (ε'') versus log (frequency) of PANI films prepared by the solution-doping method with different dopant–solvent combinations. PANI–CSA was prepared both from NMP and *m*-cresol, while PANI–DBSA was prepared both from NMP and xylene. NMP was recognized as the traditional solvent for PANI only in the insulating EB form. However, functionalized protonic acids like CSA and DBSA have been found to make PANI soluble in the conducting emeraldine salt form in common organic solvents.[27,28] Researchers also have reported that choices of dopant–solvent combinations affect profoundly the resulting conductivity of the films. Therefore, we chose *m*-cresol for PANI–CSA and xylene for PANI–DBSA, these being known as good solvents for the respective PANI–dopants in order to compare the solvent effect on the dielectric behavior of the respective PANI complexes.

The presence of a plateau in ε' and well-defined loss peak in ε'' cannot be observed in the case of PANI–DBSA. The spectra of PANI–CSA [Fig. 6(a,b)] are like those of PANI salt made from the film-doping method, while the spectra of PANI–DBSA are different from those prepared by the film-doping method. Both the ε' and ε'' values of PANI–CSA made from *m*-cresol are higher than are those made from NMP. ε'' maximum is also located in the higher-frequency region when made from the *m*-cresol solution. There is no plateau region or peak maximum in ε'' of PANI–DBSA from both solvents, and they only form a decreasing pattern with increasing frequency.

The strong low-frequency dispersions for ε' and the absence of a loss peak for ε'' are characteristic of charged carrier systems.[20] The localized charge carriers, under the applied alternating electric field, can hop to neighboring localized sites, like the reciprocating motion of a jumping dipole, or jump to neighboring sites which form a continuous connected network, allowing the charges to travel through the entire physical dimensions of the samples. The decrease of ε'' with the frequency is lower in the case of samples prepared from xylene than from NMP. The measured *s* values using eq. (2) are 0.82, 0.74, 0.29, and 0.60, respectively, for PANI–CSA from *m*-cresol and NMP and for PANI–DBSA from xylene and NMP. The *s* values of the PANI complexes (PANI–CSA and PANI–DBSA) prepared both from NMP are not much different, while those of samples prepared from other solvents, that is, xylene and *m*-cresol, have a much larger gap. The measured *s* value is, therefore, largely different for the sol-

vent used in the case of PANI–DBSA. The lowest value of the exponent s of PANI–DBSA from xylene may originate from an enhanced conduction process in this material, that is, tunneling and a hopping conduction mechanism may be due to a peculiar chain structure such as a layered structure of PANI–DBSA from xylene.[29] This structure would contribute to a self-assembled morphology, resulting in an interconnected network structure. Hence, electrical conduction would occur more easily. The layered structure seems to be heavily dependent on the solvents, that is, the selection of the solvent is a major factor in solution processing with functionalized protonic acids. The ε'' maximum was evident only in the case of PANI–CSA in our experimental region. From these experimental results, it is also concluded that different physical and chemical environments, that is, the chain structure and the dopant, contribute significantly to the dielectric relaxation behavior.

M' and M'' of solution-doped PANI films are shown in Figure 7(a,b), respectively. M' and M'' increased abruptly with increasing frequency. In Figure 7(b), the M'' of PANI–DBSA (xylene) shows a nonmonomodal distribution of the electric modulus although the higher-frequency region could not be found because of the limitation of the measurement region. This may also be due to the complicated conduction process or various phases. But, in other samples, this multiple conduction process was not present. It may be due to limitations of the measurement system or it may not happen. When m-cresol and xylene were used for preparing PANI-complex films, respectively, for PANI–CSA and PANI–DBSA, the M″ increased more slowly. M″ variation with the sample is ascribed to different conduction conditions such as the conjugation state, chain structure, and doping level stemming from different dopant–solution combinations. Therefore, the proper selection of dopant–solvent combinations would supply suitable application of conductive polymers.

Figure 8(a) reveals the complex planes for the electric modulus of solution-doped films. This does not form semicircles, which would correspond to the idealized Debye model with a single relaxation time. The skew-type behavior can probably be understood both from the conduction of various charge carriers and their resulting dipole.[10] It is most prominent in the measured frequency range in PANI–DBSA prepared from NMP. From these results, it can again be confirmed that the conduction behavior of PANI could be varied by the solution-doping method.

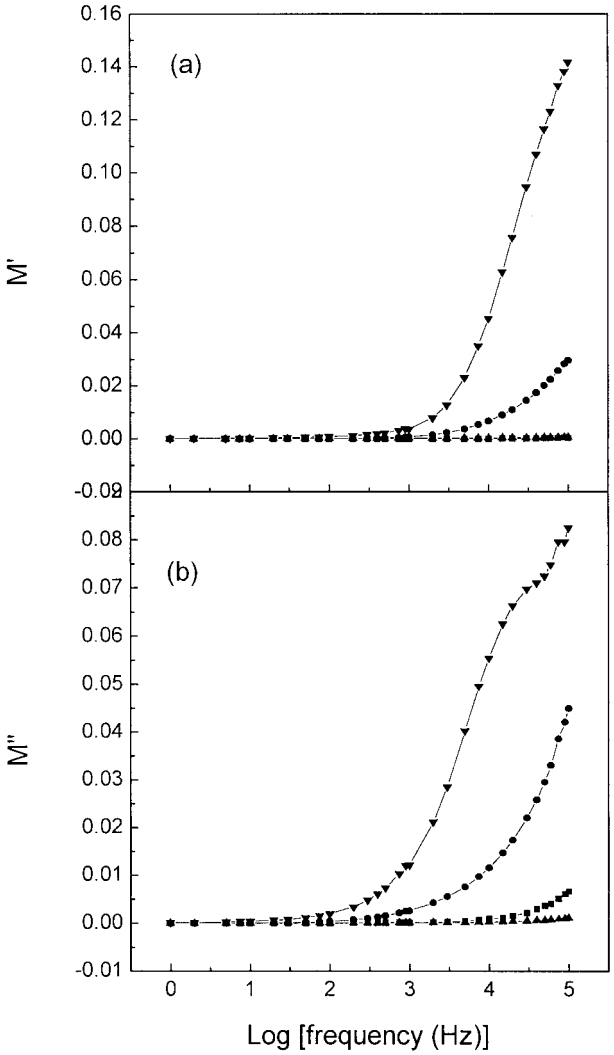

Figure 7 Electric modulus of (a) real part (M') and (b) imaginary part (M'') versus frequency for solution-doped PANI with (■) CSA–m-cresol, (●) CSA–NMP, (▲) DBSA–xylene, and (▼) DBSA–NMP.

The tan δ curves shown in Figure 8(b) can offer the prediction of dc conductivity differences in the samples. PANI–CSA shows a higher tan δ value than that of PANI–DBSA and the tan δ maximum of PANI–CSA film made from m-cresol is located at a higher frequency than that from NMP, which coincides with prediction. In case of PANI–DBSA, the tan δ maximum of the film made from NMP cannot be observed in the measured frequency range.

Figure 9 shows wide-angle X-ray diffraction (WAXD) patterns of PANI–CSA prepared from m-cresol and PANI–DBSA from xylene. The chain structures of the two samples are greatly different. In PANI–DBSA, a low-angle peak is revealed

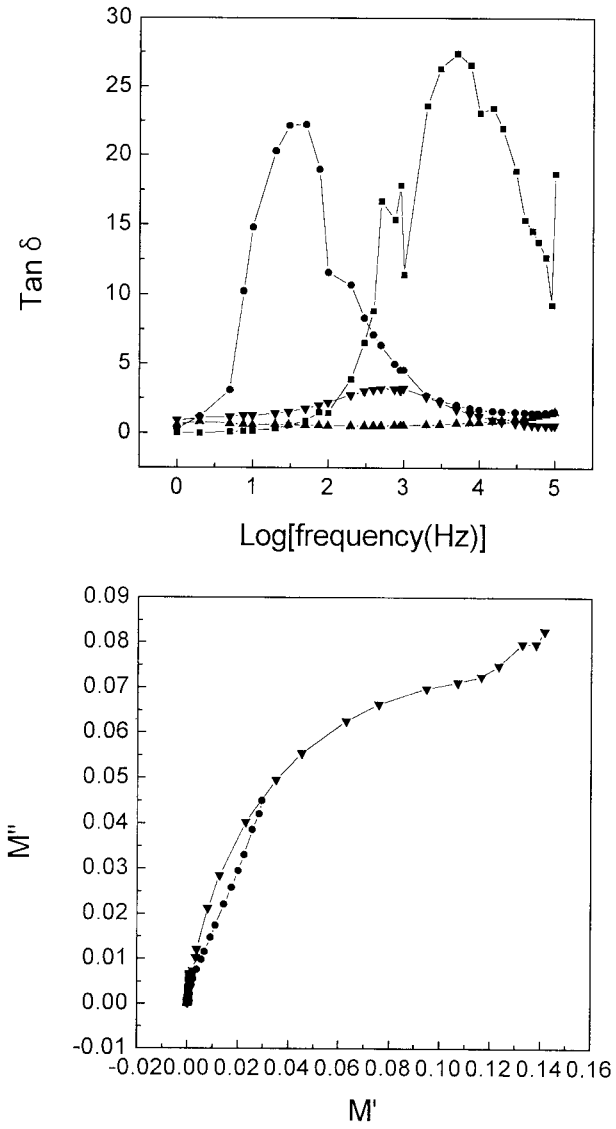

Figure 8 (a) Complex plane for the electric modulus of solution-doped PANI with (■) CSA–[*m*-cresol], (●) CSA–NMP, (▲) DBSA–xylene, and (▼) DBSA–NMP. (b) Tan δ of the same samples.

near $2\theta = 2.5°$, due to a well-defined layered structure originating from packing of the main chain into the platelike layers due the long alkyl chain of the DBSA.[29] PANI–CSA shows crystalline peaks at $2\theta = 7.8°$, 14.9°, and 24.4°, which are (002), (100), and (040) reflections, respectively.[30] This result confirms that the chain structures of PANI salts are greatly influenced by the solvent–dopant combinations in the solution-doping process. This difference in the chain structure, therefore, affects the divergence of the dielectric spectra and the *s* value.

CONCLUSIONS

The dielectric spectra of PANI salt films were analyzed by changing the dopants and film-formation methods. In the film-doping method, the increase in dopant size results in subsequent displacement of the dielectric relaxation peak toward lower frequency, which was found to be the result of an increased interchain distance on the PANI surface, leading to lowered carrier hopping. In the electric modulus formalism, the observed *M″* peak maximum was moved from about 10 Hz, in the case of PANI–EB, to about 10 MHz (PANI–HCl) depending on the dopant size. The electric conduction seemed to occur in a simple way, as suggested by the complex plane spectra of the electric modulus. The measured *s* values were similar irrespective of the dopants, indicating similar doping levels on the surface of PANI salts regardless of the dopants. In the solution-doped PANI, the dielectric spectra were changed with the selections of the dopant–solvent combinations as well as the kinds of dopants. PANI–DBSA showed different patterns of the spectra and a low *s* value, which were dependent on the peculiar

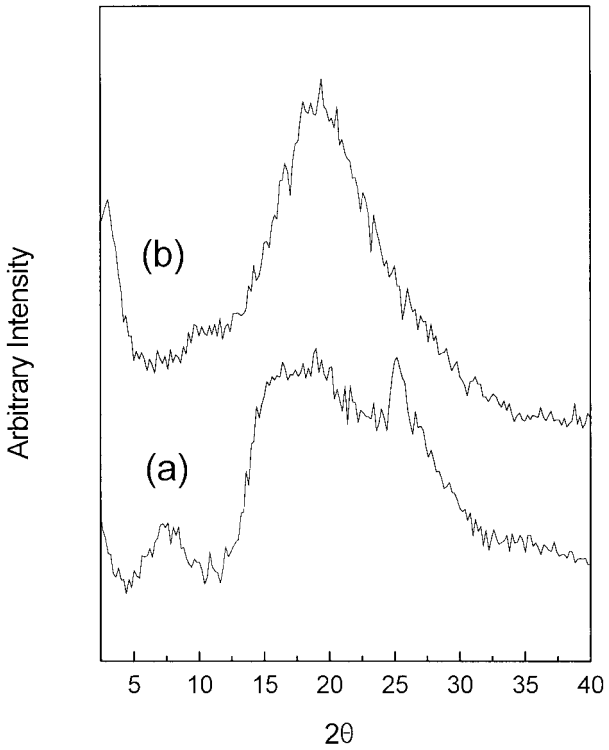

Figure 9 WAXD patterns of solution-doped PANI prepared from (a) CSA–[*m*-cresol] and (b) DBSA–xylene.

layered chain structure. The structure led to a nonmonomodal distribution of the electric modulus curves due to a complicated conduction process or various phases.

The authors gratefully thank the Center for Advanced Functional Polymers of the Engineering Research Center in the Republic of Korea for generous financial support.

REFERENCES

1. Matsunaga, T.; Daifuku, H.; Nakajima, T.; Gawagoe, T. Polym Adv Tech 1990, 1, 3.
2. Olcani, A.; Abe, M.; Ezoe, M.; Doi, T.; Miyata, T.; Miyake, A. Synth Met 1993, 57, 3969.
3. Gregory, R. V.; Himbrell, W. C.; Kuhn, H. J Coat Fabr 1991, 20, 1.
4. Gustafsson, G.; Cao, Y.; Treacy, G. M.; Klavetter, F.; Colaneri, N.; Heeger, A. J. Nature 1992, 357, 477.
5. Pinto, N. J.; Shah, P. D.; Kahol, P. K.; McCormick, B. J. Solid State Commun 1996, 97, 1029.
6. Singh, R.; Narula, A. K.; Tandon, R. P. Synth Met 1996, 82, 63.
7. Mateeva, E. S.; Calleza, R. D.; Parkhutic, V. P. Electrochim Acta 1996, 41, 1351.
8. Singh, R.; Arora, V.; Tandon, R. P.; Mansingh, A.; Chandra, S. Synth Met 1999, 104, 137.
9. Capacciooli, S.; Lucchesi, M.; Rolla, P. A.; Ruggeri, G. J Phys Condens Mater 1998, 10, 5595.
10. Ram, M. K.; Annapoorni, S.; Pandey, S. S.; Malhotra, B. D. Polymer 1998, 39, 399.
11. Kivelson, D. Phys Rev B 1987, 25, 3799.
12. Travers, J. P.; Guyadec, P. L.; Adams, P. N.; Laughlin, P. J.; Monkman, A. P. Synth Met 1994, 65, 159.
13. Zuo, F.; Angelopoulos, M.; MacDiarmid, A. G.; Epstein, A. J. Phys Rev B 1989, 39, 3570.
14. Epstein, A. J.; MacDiarmid, A. G. Makromol Chem Makromol Symp 1991, 51, 217.
15. Angelopoulos, M.; Ray, A.; MacDiarmid, A. G.; Epstein, A. J. Synth Met 1987, 21, 21.
16. Han, M. G.; Im, S. S. J Appl Polym Sci 1998, 67, 1863.
17. Han, M. G.; Im, S. S. J Appl Polym Sci 1999, 71, 2169.
18. Wei, Y.; Jang, G. W.; Hsueh, K. F.; Scherr, E.; MacDiarmid, A. G.; Epstein, A. J. Polymer 1992, 33, 314.
19. Matveeva, E. S. Synth Met 1996, 79, 127.
20. Lian, A.; Besner, S.; Dao, L. H. Synth Met 1995, 74, 21.
21. Hourquebie, P.; Olemo, L. Synth Met 1994, 65, 19.
22. He, P.; Qian, X.; Li, C. Synth Met 1993, 55–57, 5008.
23. Macedo, P. B.; Moynihan, C. T.; Bose, R. Phys Chem Glasses 1972, 13, 171.
24. Ram, M. K.; Annapoorni, S.; Pandey, S. S.; Malhotra, B. D. Polymer 1998, 39, 3399.
25. Lee, H. T.; Chuang, K. R.; Chen, S. A.; Wei, P. K.; Hsu, J. H.; Fann, W. Macromolecules 1995, 28, 7645.
26. Lee, H. T.; Liao, C. S.; Chen, S. A. Makromol Chem 1993, 194, 2443.
27. Cao, Y.; Smith, P.; Heeger, A. J. Synth Met 1992, 48, 91.
28. Beyer, G.; Steckenbiegler, B. Synth Met 1993, 60, 169.
29. Prosa, T. J.; Winokur, M. J.; Moulton, J.; Smith, P.; Heeger, A. J. Macromolecules 1992, 25, 436.
30. Djurado, D.; Gilles, B.; Ramnou, P.; Travers, J. P. Synth Met 1999, 101, 803.